Biointerface Research in Applied Chemistry
Open-Access Journal (ISSN: 2069-5837)

Article
Volume 15, Issue 1, 2025, 6
https://doi.org/10.33263/BRIAC151.006

Combined Experimental and Theoretical Studies of the 1,3-Dipolar Cycloaddition Reaction Between Phenyldiazomethane and 4-Methylthioaurone

Mohamed Bakhouch [1,*], Bouchra Es-Sounni [1], Ayoub Mouhib [1,*], Bouchra Rossafi [2], Abdelhak Ouled Aitouna [3], Samir Chtita [2], Noureddine Mazoir [1], Ahmed Benharref [3], Ghali Al Houari [4], Mohamed El Yazidi [4]

[1] Bioorganic Chemistry Team, Faculty of Science, Chouaïb Doukkali University, P.O. Box 24, 24000 El Jadida, Morocco; bakhouch.m@ucd.ac.ma;
[2] Laboratory of Analytical and Molecular Chemistry, Faculty of Sciences Ben M'Sik, Hassan II University of Casablanca, P.O. Box 7955 Casablanca, Morocco; samirchtita@gmail.com;
[3] Laboratory of Natural Substances Chemistry, Faculty of Sciences Semlalia, Cadi Ayyad University, P.O. Box 2390, 40000, Marrakech, Morocco; a.benharref@gmail.com;
[4] Engineering Laboratory of Organometallic, Molecular Materials and Environment, Faculty of Sciences Dhar EL Mahraz, Sidi Mohamed Ben Abdellah University, P.O. Box 1796 (Atlas), 30000 Fez, Morocco; elyazidimohamed@hotmail.com;
* Correspondence: bakhouch.m@ucd.ac.ma;

Scopus Author ID 38761061800
Received: 26.09.2024; Accepted: 2.01.2025; Published: 12.02.2025

Abstract: This research paper describes the synthesis of new spiropyrazoline bearing a 1-pyrazoline framework. In literature, only a few research works are devoted to synthesizing 1-pyrazoline heterocycle since this heterocycle undergoes spontaneous isomerization to its 2-pyrazoline isomeric form. Herein, the spiro 1-pyrazoline has been synthesized from thioaurone derivative through a regiospecific 1,3-dipolar cycloaddition (1,3-DC) with phenyldiazomethane. The structure of the obtained stable 1-pyrazoline has been established using IR and (^{1}H and ^{13}C) NMR spectroscopy and corroborated by mass spectrometry. Furthermore, the reaction's mechanism and regioselectivity have been investigated using DFT calculations at the B3LYP/6-31G(d) level. The outcomes have shown that the formation of the regioisomer **5** is more favorable than **5'**, which is in good agreement with the observed regioselectivity.

Keywords: 1-pyrazoline; thioaurone; phenyldiazomethane; 1,3-dipolar cycloaddition; regioselectivity; DFT.

1. Introduction

The diverse range of applications of heterocyclic compounds makes them important in many domains, especially in medicinal chemistry [1,2]. Pyrazoline is a heterocyclic compound bearing two contiguous nitrogen atoms inside the five-membered ring with one endocyclic double bond. Based on the position of the double bond, we found three different isomeric forms, namely 1-pyrazoline, 2-pyrazoline, and 3-pyrazoline (Figure 1) [3]. Recently, many studies have raised the biological potential of pyrazoline [4]. A literature survey has shown that pyrazoline possesses a large array of biological activity, such as antimicrobial [5–7], antiamoebic [8,9], anti-inflammatory [10], anticancer [11,12], antidepressant [13], steroidal [14], antiviral [15], etc.

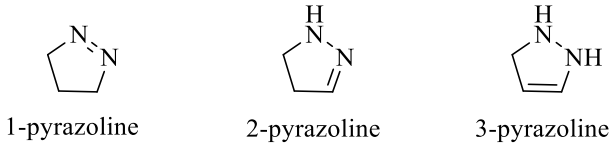

Figure 1. Structures of pyrazoline isomers.

Pyrazoline nucleus is widely found in naturally occurring compounds like alkaloids [16]. It's also found in diverse synthetic bioactive compounds [17]. In fact, literature shows that access to this heterocycle can be achieved by several methods [18]. Among the published strategies for synthesizing pyrazoline heterocycle, 1,3-DC reactions are remarkable ways to provide good selectivity, environmental, and reasonable chemical processes [19]. Depending on the targeted isomer of pyrazoline nitrile imines, diazo compounds can be used as dipoles towards olefins in 1,3-dipolar cycloaddition reactions. Despite the fact that 2-pyrazoline is the most studied isomer, a few reported works devoted to the preparation of 1-pyrazoline were found [20–23]. The 1,3-DC reaction of diazo compounds with olefins is known as a method that can lead to 1-pyrazoline, which can be isomerized spontaneously to 2-pyrazoline [24,25].

Besides, thioaurone derivatives such as α,β-unsaturated ketones bearing an exocyclic double bond have been the focus of several research studies. Their biological activity has not yet been deeply studied. A few conducted studies have shown that they were tested for their anti-cancer activity [26,27] and also for their 12/15-lipoxygenase inhibitory [28]. In addition, thioaurones are derivatives of the indigo compound, known for over a century as chromophores and dyes [29,30]. Due to their conformational orientation properties, thioaurones are considered photoswitches. This property makes them highly interesting compounds [31]. Moreover, thioaurones are widely used as starting materials to create new compounds with high added value [32,33].

During our ongoing research on the development of new heterocycles with biological interest [34–38], the aim of the current paper is the synthesis of an undescribed 1-pyrazoline derivative from 4-methylthioaurone and phenyldiazomethane. We have also conducted a DFT study of the mechanism of the involved reaction.

2. Materials and Methods

2.1. General.

All chemicals were of analytical grade and were utilized directly, with no further purification. Melting points were determined using a previously calibrated KOFLER Bench, with an uncertainty of ±2°C. A Thermo Scientific TM Nicolet iS10 FT-IR spectrometer was used to record IR spectra. A BRUKER AVANCE II spectrometer (300 MHz for ^{1}H and 75 MHz for ^{13}C) was used to record NMR spectra in the appropriate solvent mentioned in the experimental section. The APT sequence was used to record ^{13}C NMR spectra. The advancement of the reaction was monitored using silica gel TLC plates (Merck 60 F254, thickness: 0.2 mm), and the spots were visualized with a UV lamp (254-365 nm). A Waters® Acquity^{TM} Ultra Performance LC system coupled to an AcquityTM triple quadrupole (Waters®, Ireland) was equipped with an electrospray ionization (ESI) to record HRMS spectra.

2.2. General synthetic procedures.

2.2.1. 2-[(Carboxymethyl)sulfanyl]benzoic acid **1**.

In a 500 mL two-neck flask fitted with a condenser containing 250 mL of water, 0.065 mol of thiosalicylic acid, 0.25 mol of sodium carbonate, and 0.065 mol of monochloroacetic acid was dissolved. The mixture was heated at reflux for 4 hours, then activated carbon (1g) was added, and the refluxing was continued for 10 min. After filtration, hydrochloric acid (12 N) was added to the mixture until pH = 1. The obtained precipitate was collected by filtration, rinsed thoroughly with cold water, and recrystallized in ethanol.

White solid, Yield = 77%, m.p. = 210 °C. ^{1}H NMR (300 MHz, DMSO-d_6, δ in ppm): 3.81 (s, 2H, CH_2), 7.72 (td, 1H, $^{3}J_o$ = 7.7 Hz, $^{4}J_m$ = 0.8 Hz), 7.36 (dd, 1H, $^{3}J_o$ = 7.7 Hz, $^{3}J_4$ = 0.8 Hz), 7.53 (td, 1H, $^{3}J_o$ = 7.4 Hz, $^{4}J_m$ = 1.5 Hz), 7,91 (dd, 1H, $^{3}J_o$ = 7.4 Hz, $^{4}J_m$ = 1.5 Hz), 12.94 (s, 2H, -COOH). ^{13}C NMR (75 MHz, DMSO-d_6, δ in ppm): 34.4 (S-CH_2), 124.5, 125.7, 128.1 (C_1), 131.4, 132.9, 140.8 (C_2), 167.8 (C_1-COOH), 171.1 (CH_2-COOH).

2.2.2. Synthesis of 3-acetoxybenzothiophene **2**.

A mixture of **1** (0.05 mol), acetic anhydride (80 ml), and acetic acid (20 ml) was introduced in a 100 mL flask equipped with a condenser and a stir bar. Then, the mixture was heated for one hour under magnetic stirring, and acetic anhydride was distilled off under vacuum. The obtained crude was transferred to a separatory funnel containing 60 mL of water and extracted with diethyl ether (3 x 20 mL). The organic layers were gathered and dried over anhydrous sodium sulfate Na_2SO_4 after filtration and elimination of the solvent using a rotary evaporator. The crude material was purified by silica gel column chromatography using a mixture of hexane/ether (4:1) to give a pure product.

Red oil, Yield = 70 %, ATR-IR: 1764 cm^{-1} (C=O). ^{1}H NMR (300 MHz, $CDCl_3$, δ in ppm): 7.41-7.86 (m, 4H, H_{Ar}), 7.46 (s, 1H, $H_{ethylenic}$), 2.41 (s, 3H, $COCH_3$). ^{13}C NMR (75 MHz, $CDCl_3$, δ in ppm): 21.0 (CH_3), 111.9 (C_2), 120.5, 122.9, 124.4, 125.2, 132.2, 136.9, 140.8 (C_3), 168.3 (C=O).

2.2.3. Synthesis of (Z) 2-(4-methylbenzylidene)benzo[b]thiophen-3(2H)-one **3**.

An aqueous solution of sodium hydroxide (2N) (50 mL) was placed in a three-neck flask fitted with a condenser, a nitrogen bubbler, and a dropping funnel. The solution was bubbled for 2 to 3 minutes by a nitrogen stream, and 3-acetoxybenzothiophene **2** (20 mmol) was added under magnetic stirring for 20 min. Then, 4-methyl benzaldehyde (20 mmol) dissolved in ethanol (4 mL) was slowly dropwise under vigorous stirring until the formation of a yellow solid, which was isolated by filtration, washed thoroughly with cold water and recrystallized in ethanol.

Yellow solid, Yield = 86%, m.p. = 144 °C. ATR-IR: 1679 cm^{-1} (C=O), 1580 cm^{-1} (C=C). ^{1}H NMR (300 MHz, $CDCl_3$, δ in ppm): 7.95 (s, 1H, $H_β$), 7.93 (d, 1H, $^{3}J_o$ = 6.8 Hz), 7.61 (d, 2H, ^{3}J = 8.7 Hz), 7.55 (dd, 1H, $^{3}J_o$ = 6.9 Hz, $^{4}J_m$ = 1.3 Hz), 7.49 (d, 1H, $^{3}J_o$ = 7.7 Hz), 7.32-7.26 (m, 3H, H_{Ar}), 2.41 (s, 3H, CH_3). ^{13}C NMR (75 MHz, $CDCl_3$, δ in ppm): 21.6, 123.8, 125.5, 126.9, 129.2, 129.8, 130.3, 130.6, 131.0, 131.5, 133.1, 133.7, 135.1, 140.8, 146.1, 188.6 (C=O).

2.2.4. Synthesis of spiro-1-pyrazoline **5**

4-methylthio aurone **3** (0.55 mmol), tosylhydrazone **4** (1.1108 mmol), and cesium carbonate Cs_2CO_3 (1.1108 mmol) were introduced in a 100 mL flask, fitted with a condenser containing 1,4-dioxane (20 mL). Then, the reaction mixture was heated at reflux under magnetic stirring for 4 hours. Diluted with water (20 mL) and extracted using dichloromethane (3 x 20 mL). The organic layers were gathered and distilled to remove the solvent. The obtained crude product was purified using silica gel column chromatography and a mixture of hexane/ethyl acetate as eluent.

White powder, Yield = 52%, m.p. = 95 °C. ATR-IR: 3025 cm^{-1} (=C-H); 2919 cm^{-1} (-C-H), 1669 cm^{-1} (C=O); 1590, 1515, 1497, 1448 cm^{-1} (C=C-C=C). ^{1}H NMR (300 MHz, $CDCl_3$, δ in ppm): 2.43 (s, 3H, CH_3), 3.87 (d, 1H, CH, ^3J = 9.32 Hz), 3.94 (d, 1H, CH, ^3J = 8.98 Hz), 7.20-7.56 (m, 12H, H_{Ar}), 7.72 (d, 1H, H_{Ar}, ^3J = 7.81 Hz). ^{13}C NMR (75 MHz, $CDCl_3$, δ in ppm): 21.29 (CH_3), 38.63 (C_4), 41.08 (C_3), 51.98 (C_5), 123.95, 124.67, 126.14, 127.62, 128.20, 128.30, 129.45, 129.60, 131.24 (C_q-CO), 133.45 (C_q), 134.47, 137.74 (C_q-CH_3), 151.24 (C_q-S), 195.65 (C=O). HRMS (ESI+): calcd for $[M+H]^+$: 371.1218, found: 371.0065.

2.3. DFT study.

The described 1,3-DC reaction between 4-methylthioaurone and phenyldiazomethane has been subject to a theoretical using the Density Functional Theory (DFT) method. The calculations have been conducted employing the B3LYP [39] functional conjointly with the 6-31G(d) basis set [40]. Berny analytical gradients method has been employed to optimize the structure of the involved chemicals in this study [41]. Frequency computations have been performed to characterize the stationary points, ensuring that transition states (**TSs**) exhibit precisely one imaginary frequency. The intrinsic reactions coordinate [42] (IRC) paths have been drawn to illustrate the energy profiles connecting each transition state (**TS**) to the two related minima [43]. The Gaussian 09 software suite has been used to perform all the calculations [44], and the Gauss View 6.0 software has been used for the visualization of all molecular structures as well as the calculation results. The expression $\omega = (\mu^2/2\eta)$ has been used to give the electrophilicity indices ω [45]. The energies of the frontier molecular orbitals E_{HOMO} and E_{LUMO} have been used to determine the electronic chemical potential (μ) and the chemical hardness (η) as follows $\mu = (E_{HOMO} + E_{LUMO})/2$, and $\eta = (E_{LUMO} - E_{HOMO})$, respectively [46]. Furthermore, the obtained HOMO energy within the Kohn-Sham [48] has been used to introduce the empirical nucleophilicity index N [47] as $N = E_{HOMO}(Nu) - E_{HOMO}(TCE)$. The nucleophilicity has been compared to tetracyanoethylene (TCE), which exhibits the lowest HOMO energy among a broad range of previously studied organic molecules [47]. This choice allowed us conveniently to handle a nucleophilicity scale of positive values.

3. Results and Discussion

3.1. Synthesis.

The starting material 4-methylthioaurone **3**, its IUPAC name is (Z)-2-(4-methylbenzylidenebenzo[b]thiophen-3(2H)-one, has been prepared using our previously published procedure [49,50]. The procedure starts with condensing thiosalicylic acid on 2-chloroacetic acid to afford 2-[(carboxymethyl)sulfanyl]benzoic acid **1**. Compound **1** has been

then subjected to Rössing decarboxylative cyclisation conditions [51] to give 3-acetoxybenzothiophene **2**. This later has been condensed with 4-menthylbenzaldehyde in the presence of sodium carbonate, leading to 4-methylthio aurone **3** in excellent yield (Scheme 1). To prevent intermediate **2** from dimerizing onto thioindigo [52], nitrogen steam has been used.

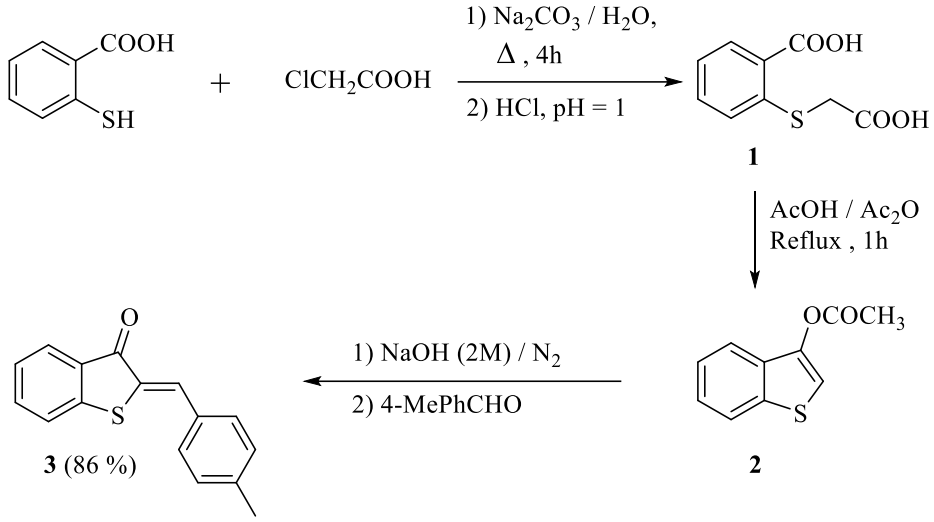

Scheme 1. Synthetic pathway of 4-methylthio aurone **3**.

The obtained 4-methylthioaurone **3** has been used as a dipolarophile in the 1,3-DC reaction with phenyldiazomethane **4**. The reaction was performed in dioxane with the existence of cesium carbonate Cs_2CO_3 as a catalyst to give spirocycloadduct **5** encompassing 1-pyrazoline nucleus (Scheme 2). The reaction occurs in a regiospecific way to afford only a single cycloadduct with good yield.

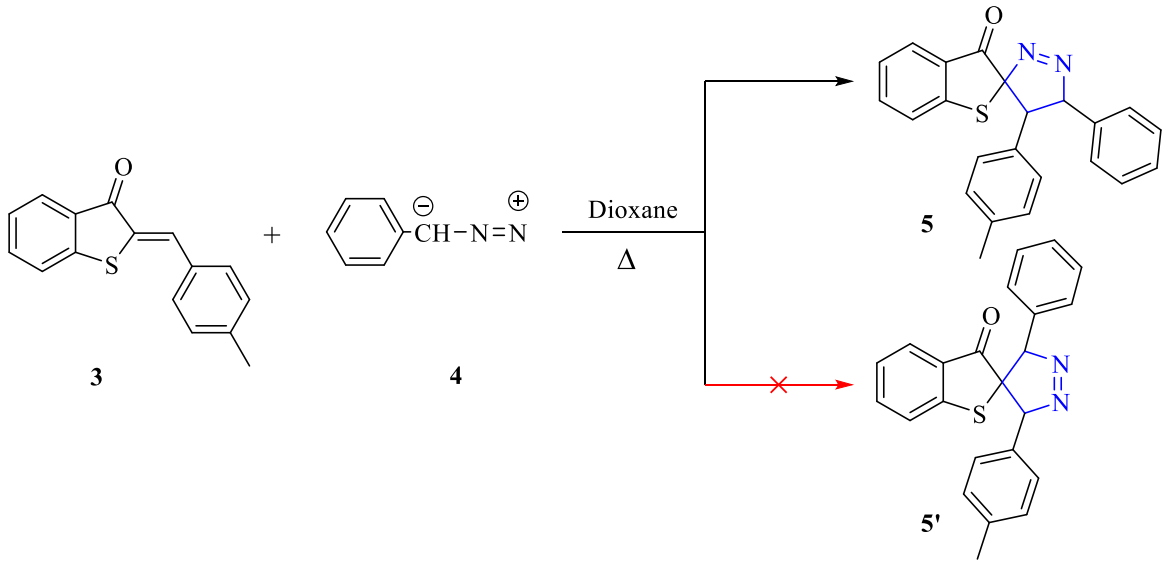

Scheme 2. Synthesis of spiro-1-pyrazoline **5**.

The phenyldiazomethane **4** used as a dipole in the 1,3-DC reaction has been produced *in situ* using a previously reported method [53] by the action of cesium carbonate on tosylhydrazone precursor through the pathway depicted in scheme 3.

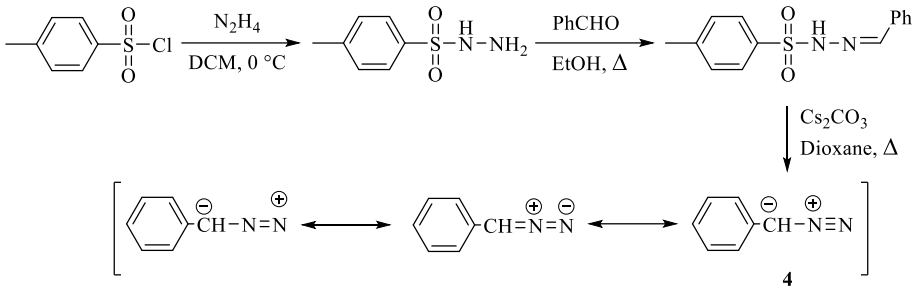

Scheme 3. Synthesis of phenyldiazomethane **4**.

3.2. Spectroscopic characterization.

The obtained spirocycloadduct **5** has been identified using spectroscopic techniques, such as IR, (^{1}H and ^{13}C) NMR, and corroborated by mass spectrometry. The infrared spectrum of the spirocycloadduct **5** (Figure 2) shows the presence of a band at 3025 cm^{-1}, which corresponds to the stretching of the aromatic C-H bonds, and a strong band at 1669 cm^{-1} attributable to the stretching of the carbonyl group (C=O). It also displays four bands belonging to the stretching of the aromatic skeleton (C=C-C=C) at a range of 1448-1590 cm^{-1}.

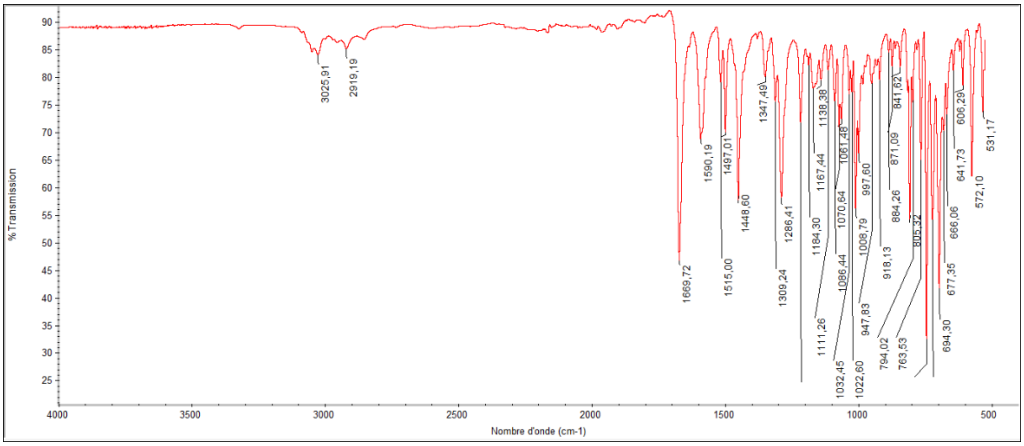

Figure 2. ATR-IR spectrum of spiropyrazoline **5**.

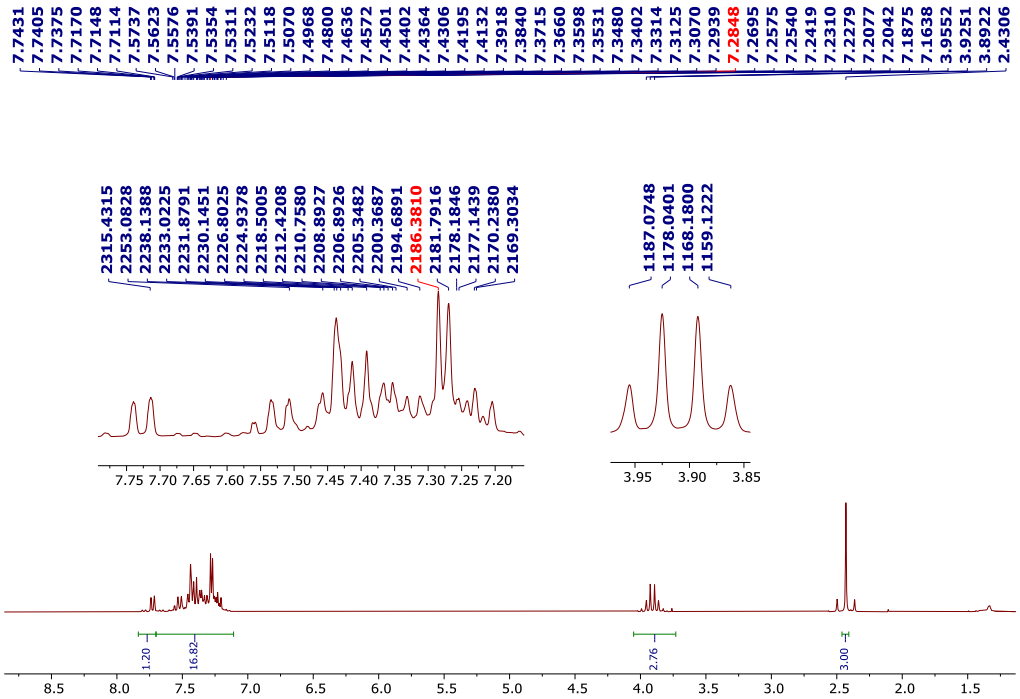

Figure 3. ^{1}H NMR (300 MHz, $CDCl_3$) spectrum of spiropyrazoline **5**.

The ^{1}H NMR spectrum of compound **5** (Figure 3) recorded in $CDCl_3$ reveals in addition to signals attributable to aromatic protons, a singlet signal at 2.43 ppm integrates 3 protons assigned to the methyl protons. The spectrum exhibits two doublet signals centered at 3.87 and 3.94 ppm relative to the two methine protons of the pyrazoline ring, forming an AB system with a coupling constant of 9 Hz attesting to an anti-disposition. The proton NMR data are in favor of the regioisomer **5**. In addition, the absence of singlet signals that could be attributed to the protons of the two methine groups favors the observed regiochemistry.

Its ^{13}C NMR spectrum (Figure 4) shows the existence of the following characteristic signals: a signal at 21.29 ppm assigned to the methyl carbon. Carbons of the two methine groups at positions 4 and 3 of the pyrazoline ring resonate at 38.63 and 41.08 ppm, respectively. The signal of the spiranic quaternary carbon (C_5) appears at 51.98 ppm. The signal 195.65 ppm is attributable to the carbon of the carbonyl group.

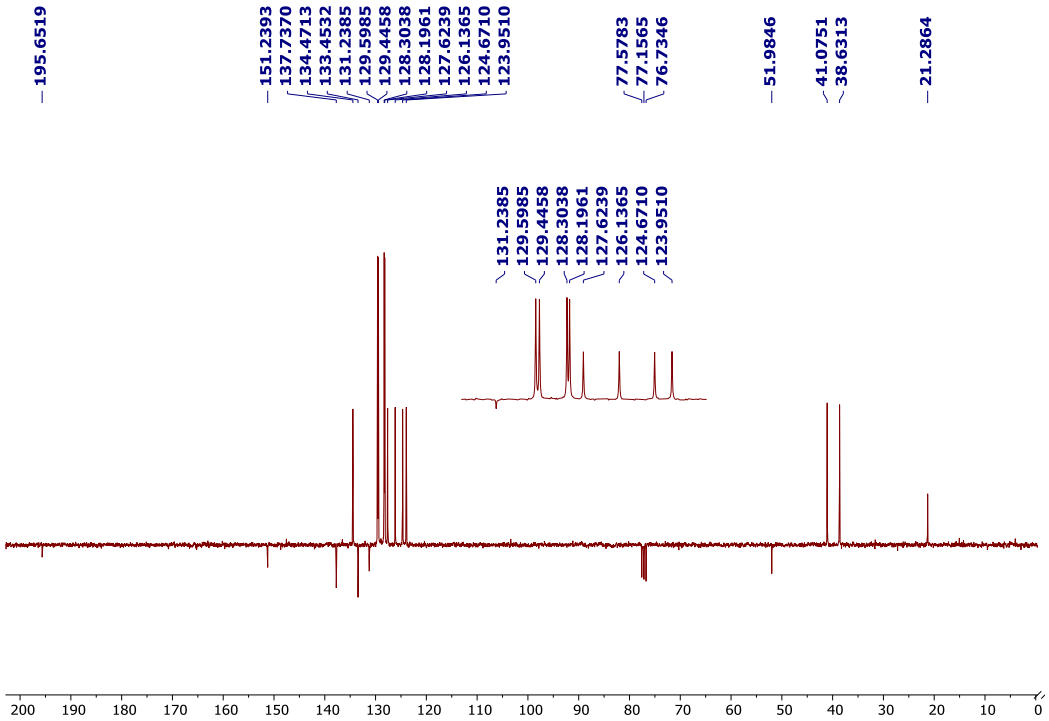

Figure 4. ^{13}C-APT NMR (75 MHz, $CDCl_3$) spectrum of spiropyrazoline **5**.

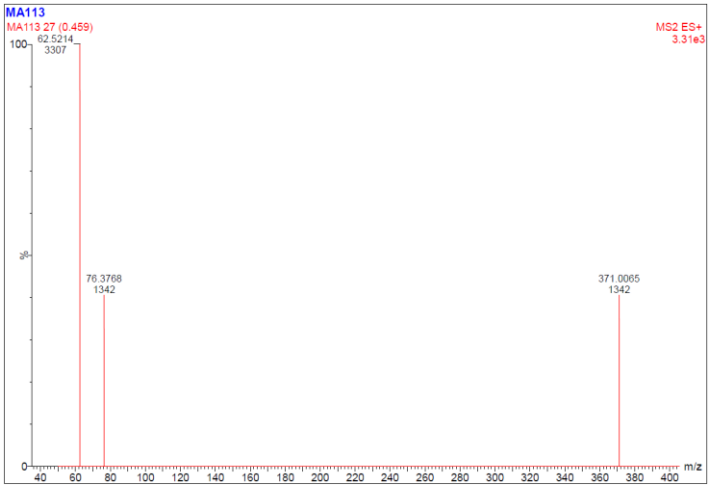

Figure 5. ESI+ spectrum of spiropyrazoline **5**.

The structure of the synthesized spiro-1-pyrazoline has been further confirmed by mass spectrometry. The ESI+ spectrum of the spirocycloadduct **5** (Figure 5) shows a molecular peak at 371.0065 Da, belonging to the exact mass of the proposed structure.

3.3. Theoretical study.

3.3.1. Global reactivity indices.

With the aim of giving more insight into the mechanism of the described 1,3-DC reaction between the thioaurone derivative and phenyldiazomethane, as well as predicting the behavior of synthons, we have conducted a theoretical study. For this reason, the global indices chemical potential (μ), chemical hardness (η), electrophilicity (ω), and nucleophilicity (N) have been calculated for reagents involved in the investigated 1,3-DC reaction. The obtained outcomes are listed in Table 1.

Table 1. B3LYP/6-31G(d) electronic chemical potential μ, chemical hardness η, electrophilicity ω, nucleophilicity N, in eV, of the two reagents.

System	μ	η	ω	N
Dipolarophile 3	−3.96	3.40	2.30	3.46
Dipole 4	−3.47	3.88	1.55	3.71

Based on the results presented in Table 1, a detailed analysis of the global indices reveals significant insights into the reactivity of compounds involved in this 1,3-DC reaction. The electronic chemical potential (μ) of dipole 4 is −3.47 eV, slightly higher than that of dipolarophile **3**, which is −3.96 eV. This indicates that during the reaction, dipole **4** is likely to donate electrons to dipolarophile **3**, suggesting a charge transfer from **4** to **3**. Additionally, the nucleophilicity and electrophilicity indices further elucidate their reactivity profiles. The dipolarophile **3** has a nucleophilicity index (N) and an electrophilicity index (ω) values of 3.46 eV and 2.30 eV, respectively, while the dipole **4** exhibits slightly higher nucleophilicity (3.71 eV) but a lower electrophilicity (1.55 eV). Therefore, the reactivity pattern suggests that synthon **4** is more likely to act as a nucleophile, while synthon **3** is predisposed to function as an electrophile in the process of this reaction.

3.3.2. Energetic study.

Due to the asymmetry of both reagents, the 1,3-DC reaction between **3** and **4** can proceed via two competing pathways.

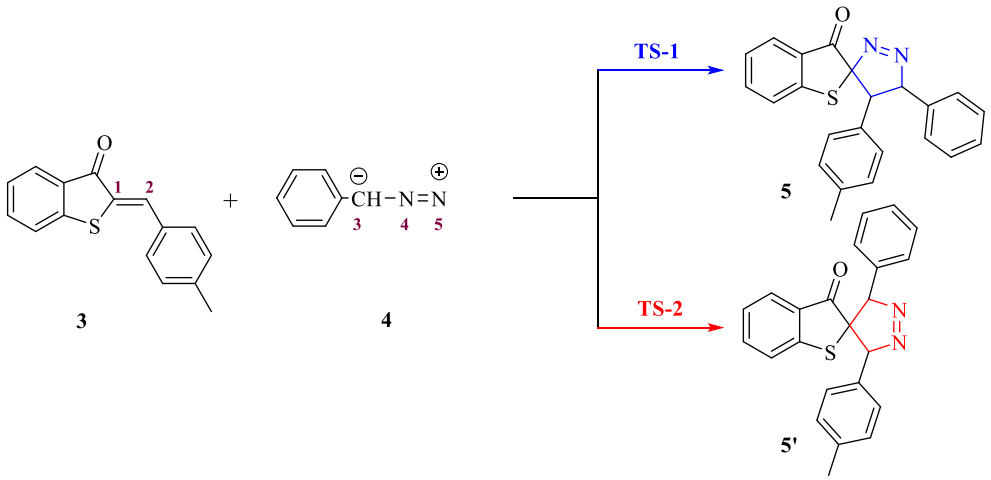

Scheme 4. Regioselective pathways of the 1,3-DC reaction between synthons **3** and **4**.

These pathways correspond to two regioisomeric modes of approach: involving the formation of single bonds C_1-N_5 and C_2-C_3 to give regioisomer **5**, or the formation of single bonds C_1-C_3 and C_2-N_5 to give regioisomer **5'**. Each pathway is associated with a distinct transition state, **TS-1,** and **TS-2**, respectively, as illustrated in Scheme 4.

The total and relative energies have been determined and listed in Table 2. The energy profiles of the reaction pathways associated with the 1,3-DC between reagents **3** and **4** are illustrated in Figure 6.

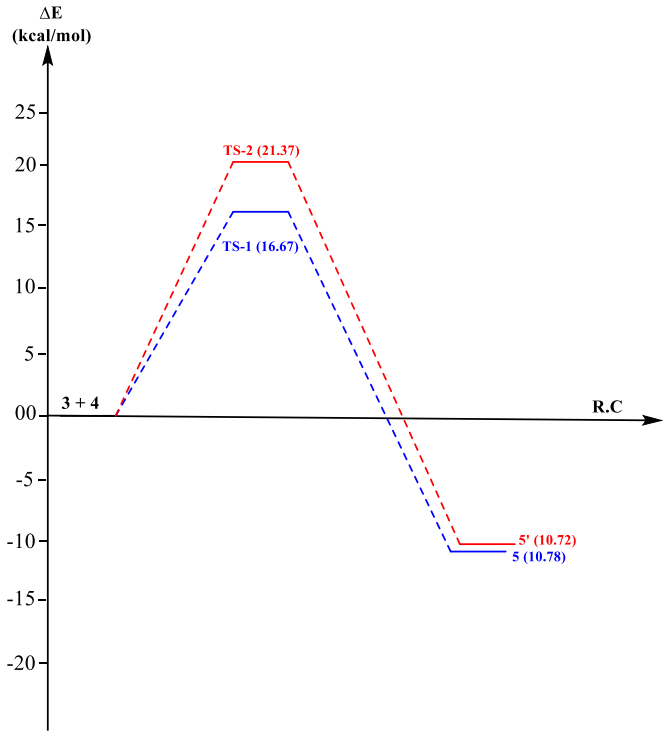

Figure 6. Energies profiles for the studied reaction paths between 3 and 4.

Based on the results presented in Table 2, the 1,3-DC reaction between **3** and **4** demonstrates an exothermic nature, forming spiro cycloadducts **5** and **5'** releasing energies of −10.78 and −10.72 kcal/mol, respectively. This exothermicity indicates that the reaction proceeds with a strong preference for product formation under kinetic control. The activation energies for the transition states **TS-1** and **TS-2** are 16.67 and 21.37 kcal/mol, respectively, highlighting that the formation of regioisomer **5** is kinetically more likely than **5'**. Consequently, regioisomer **5** not only emerges as the favored product in terms of kinetic control but also aligns with thermodynamic favorability due to its lower formation energy. This analysis is consistent with experimental observations, reinforcing that regioisomer **5** is kinetically and thermodynamically favored in this reaction process.

Table 2. B3LYP/6-31G(d) total (E, in a.u.) and relative energies (ΔE, in kcal/mol) for the species involved in the investigated 1,3-DC reaction between **3** and **4**.

System	E (u.a)	ΔE (kcal/mol)
3	−1090.352784	
4	−379.801663	
3 + 4	−1470.154447	
5	−1470.171530	−10.78
5'	−1470.171621	−10.72
TS-1	−1470.127878	16.67
TS-2	−1470.120388	21.37

Figure 7 illustrates the transition state geometries for the two reaction pathways. The analysis of these geometries reveals that in the **TS-1**, the bond lengths of the newly formed bonds C_1-N_5 and C_2-C_3 are 1.702 Å and 1.704 Å, respectively. In the **TS-2**, the bond lengths for C_1-C_3 and C_2-N_5 are 1.927 Å and 1.916 Å. These observations indicate that the formation of the new single bonds occurs asynchronously.

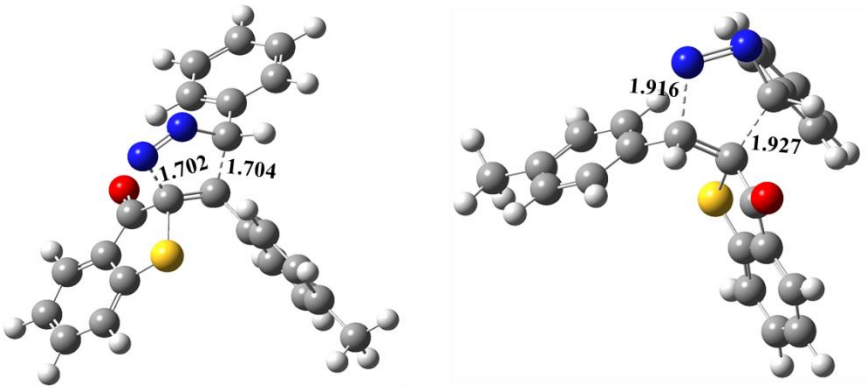

Figure 7. B3LYP/6-31G(d) geometries of the TSs involved in the regioselective reaction between **3** and **4**. Distances are given in Angstroms Å.

The Intrinsic Reaction Coordinate (IRC) curve is essential for elucidating reaction mechanisms, as it illustrates the progression of molecular structure from the reactant state to the product state via the transition state. Analysis of the IRC curve for the studied 1,3-DC reaction reveals that the reaction occurs in a concerted mechanism following the favored path (**TS-1**).

4. Conclusions

In this work, we were able to synthesize new spiro pyrazoline encompassing 1-pyrazoline moiety from thioaurone derivative and phenyldiazomethane using a 1,3-DC reaction. The spectral data are in good agreement with the proposed structure of the spiropyrazoline **5**. The data also suggest that the cycloaddition reaction proceeds in a regiospecific manner in favor of regioisomer **5**. The regioselectivity and the mechanism of this reaction were further investigated using DFT calculations at the B3LYP/6-31G(d) level. The analysis of the energy profiles indicated that the formation of both possible regioisomers **5** and **5'** is exothermic. In addition, it also revealed that regioisomer **5** is kinetically and thermodynamically more favorable rather than **5'**, which aligns well with the observed experimental results.

Funding

This research received no external funding.

Acknowledgments

The authors are thankful to Dr Manal ZEFZOUFI for her valuable input in this work.

Conflicts of Interest

The authors declare no conflict of interest.

References

1 Ravindar, L.; Hasbullah, S. A.; Rakesh, K. P.; Hassan, N. I. Pyrazole and Pyrazoline Derivatives as Antimalarial Agents: A Key Review. *Eur. J. Pharm. Sci*. **2023**, *183*, 106365, https://doi.org/10.1016/j.ejps.2022.106365.

2 Haider, K.; Shafeeque, M.; Yahya, S.; Yar, M. S. A Comprehensive Review on Pyrazoline Based Heterocyclic Hybrids as Potent Anticancer Agents. *Eur. J. Med. Chem. Rep*. **2022**, *5*, 100042, https://doi.org/10.1016/j.ejmcr.2022.100042.

3 Hoz, A. D. L.; Claramunt, R. M.; Elguero, J.; Alkorta, I. 3-Pyrazolines (2,3-Dihydro-1H-Pyrazoles): Synthesis, Reactivity, and Physical and Biological Properties. *Arkivoc* **2021**, *2021*, 75–129, https://doi.org/10.24820/ark.5550190.p011.521.

4 Shekhar Yadav, C.; Azad, I.; Rahman Khan, A.; Nasibullah, M.; Ahmad, N.; Hansda, D.; Nusrat Ali, S.; Shrivastav, K.; Akil, M.; Lohani, M. B. Recent Advances in the Synthesis of Pyrazoline Derivatives from Chalcones as Potent Pharmacological Agents: A Comprehensive Review. *Results Chem*. **2024**, *7*, 101326, https://doi.org/10.1016/j.rechem.2024.101326.

5 Murwih Alidmat, M.; Khairuddean, M.; Mohammad Norman, N.; Mohamed Asri, A. N.; Mohd Suhaimi, M. H.; Sharma, G. Synthesis, Characterization, Docking Study and Biological Evaluation of New Chalcone, Pyrazoline, and Pyrimidine Derivatives as Potent Antimalarial Compounds. *Arab. J. Chem*. **2021**, *14*, 103304, https://doi.org/10.1016/j.arabjc.2021.103304.

6 Barghady, N.; Chalkha, M.; Yamari, I.; Aflak, N.; Abchir, O.; Chebbac, K.; Nakkabi, A.; Chtita, S.; Chkirate, K.; Mague, J. T.; Mabrouk, E. H.; Baouid, A.; El Yazidi, M. Synthesis, Characterization, Mechanistic Study, in-Vitro and in-Silico Evaluation of Antibacterial and Antioxidant Activities of Novel Pyrazole-Pyrazoline Hybrid Systems. *J. Mol. Struct*. **2024**, *1309*, 138087, https://doi.org/10.1016/j.molstruc.2024.138087.

7 Mohammed Musthafa, T. N.; Snigdha, K.; Asiri, A. M.; Sobahi, T. R.; Asad, M. Green Synthesis of Chromonyl Chalcone and Pyrazoline as Potential Antimicrobial Agents – DFT, Molecular Docking and Antimicrobial Studies. *J. Mol. Struct*. **2023**, *1271*, 133993, https://doi.org/10.1016/j.molstruc.2022.133993.

8 Budakoti, A.; Abid, M.; Azam, A. Syntheses, Characterization and in Vitro Antiamoebic Activity of New Pd(II) Complexes with 1-N-Substituted Thiocarbamoyl-3,5-Diphenyl-2-Pyrazoline Derivatives. *Eur. J. Med. Chem*. **2007**, *42*, 544–551, https://doi.org/10.1016/j.ejmech.2006.10.011.

9 Bhat, A. R.; Athar, F.; Azam, A. Bis-Pyrazolines: Synthesis, Characterization and Antiamoebic Activity as Inhibitors of Growth of Entamoeba Histolytica. *Eur. J. Med. Chem*. **2009**, *44*, 426–431, https://doi.org/10.1016/j.ejmech.2007.11.005.

10 Mantzanidou, M.; Pontiki, E.; Hadjipavlou-Litina, D. Pyrazoles and Pyrazolines as Anti-Inflammatory Agents. *Molecules* **2021**, *26*, 3439, https://doi.org/10.3390/molecules26113439.

11 Katariya, K. D.; Vennapu, D. R.; Shah, S. R. Synthesis and Molecular Docking Study of New 1,3-Oxazole Clubbed Pyridyl-Pyrazolines as Anticancer and Antimicrobial Agents. *J. Mol. Struct*. **2021**, *1232*, 130036, https://doi.org/10.1016/j.molstruc.2021.130036.

12 Roman, G. Anticancer Activity of Coumarin–Pyrazoline Hybrids: A Mini-Review. *Chem. Afr*. **2024**, *7*, 2307–2319, https://doi.org/10.1007/s42250-024-00895-5.

13 Choudhary, D.; Kaur, R.; Singh, T. G.; Kumar, B. Pyrazoline Derivatives as Promising MAO-A Targeting Antidepressants: An Update. *Curr. Top. Med. Chem*. **2024**, *24*, 401–415, https://doi.org/10.2174/0115680266280249240126052505.

14 Banday, A. H.; Shameem, S. A.; Jeelani, S. Steroidal Pyrazolines and Pyrazoles as Potential 5α-Reductase Inhibitors: Synthesis and Biological Evaluation. *Steroids* **2014**, *92*, 13–19, https://doi.org/10.1016/j.steroids.2014.09.004.

15 Bai, L.; Wei, C.; Shen, Z.; He, H.; Yang, X.; Shi, S.; Hu, D.; Song, B. Splicing Indoles and 4,5-Dihydro-1H-Pyrazoline Structure Gave Birth to Novel Antiviral Agents: Design, Synthesis, and Mechanism Study. *J. Agric. Food Chem*. **2023**, *71*, 7239–7249, https://doi.org/10.1021/acs.jafc.3c01005.

16 Kadhim, E. J.; AL-Shammaa, D. A. Phytochemical Characterization Using GC-MS Analysis of Methanolic Extract of Moringa Oleifera (Family Moringaceae) Plant Cultivated in Iraq. *Chem. Mater. Res*. **2014**, *6*, 9–26.

17 Faisal, M.; Saeed, A.; Hussain, S.; Dar, P.; Larik, F. A. Recent Developments in Synthetic Chemistry and Biological Activities of Pyrazole Derivatives. *J. Chem. Sci*. **2019**, *131*, 70, https://doi.org/10.1007/s12039-019-1646-1.

18 Singh, H.; Kumar, R.; Mazumder, A. Pyrazoline and Analogs: Substrate-Based Synthetic Strategies. *Curr. Org. Synth*. **2024**, *21*, 823–836, https://doi.org/10.2174/1570179421666230822100043.

19 Singh, H.; Kumar, R.; Mazumder, A. Synthesis of Pyrazolines via 1,3-Dipolar Cycloaddition Reactions. *Synth. Commun*. **2023**, *53*, 755–770, https://doi.org/10.1080/00397911.2023.2201455.

20 Simovic, D.; Di, M.; Marks, V.; Chatfield, D. C.; Rein, K. S. 1,3-Dipolar Cycloadditions of Trimethylsilyldiazomethane Revisited: Steric Demand of the Dipolarophile and the Influence on Product Distribution. *J. Org. Chem*. **2007**, *72*, 650–653, https://doi.org/10.1021/jo061838t.

21 Impastato, F. J.; Barash, L.; Walborsky, H. M. Partial Asymmetric Synthesis in the Addition of Diphenyldiazomethane to Olefins. *J. Am. Chem. Soc*. **1959**, *81*, 1514–1515, https://doi.org/10.1021/ja01515a062.

22 Sun, H.; Wang, X.; Zhan, M.; Liu, J.; Xie, Y. Facile Synthesis of Novel Tetrasubstituted 1-Pyrazolines from Baylis–Hillman Adducts and Acyl Diazomethanes. *Tetrahedron Lett*. **2013**, *54*, 3846–3850, https://doi.org/10.1016/j.tetlet.2013.05.041.

23 Lévai, A.; Simon, A.; Jenei, A.; Kálmán, G.; Jekő, J.; Tóth, G. Synthesis of Spiro-1-Pyrazolines by the Reaction of Exocyclic α,β,γ,δ-Unsaturated Ketones with Diazomethane. *Arkivoc* **2009**, *2009*, 161–172, https://doi.org/10.3998/ark.5550190.0010.c14.

24 Jones, W. M. Pyrazolines. III. The Stereochemistry of the Decomposition of 2-Pyrazolines. *J. Am. Chem. Soc*. **1959**, *81*, 5153–5156, https://doi.org/10.1021/ja01528a033.

25 W. M. Jones; Tai, W.-T. Pyrazolines. VII. The Stereochemistry of the Thermal Decomposition of 5-Phenyl-1-Pyrazolines. *J. Org. Chem*. **1962**, *27*, 1324–1328, https://doi.org/10.1021/jo01051a048.

26 Zaher, A. F.; Abuel-Maaty, S. M.; El-Nassan, H. B.; Amer, S. A. S.; Abdelghany, T. M. Synthesis, Antitumor Screening and Cell Cycle Analysis of Novel Benzothieno[3,2-b]Pyran Derivatives. *J. Enzyme Inhib. Med. Chem.* **2016**, *31*, 145–153, https://doi.org/10.1080/14756366.2016.1222582.

27 Mouineer, A.; Zaher, A.; El-Malah, A.; Sobh, E. A.-F. Design, Synthesis, Antitumor Activity, Cell Cycle Analysis and ELISA Assay for Cyclin Dependant Kinase-2 of a New (4-Aryl-6-Flouro-4H-Benzo[4,5]Thieno[3,2-b]Pyran) Derivatives. *Mediterr. J. Chem*. **2017**, *6*, 165–179, https://doi.org/10.13171/mjc65/01709262240-zaher.

28 Herre, S.; Schadendorf, T.; Ivanov, I.; Herrberger, C.; Steinle, W.; Rück-Braun, K.; Preissner, R.; Kuhn, H. Photoactivation of an Inhibitor of the 12/15-Lipoxygenase Pathway. *ChemBioChem* **2006**, *7*, 1089–1095, https://doi.org/10.1002/cbic.200600082.

29 Baeyer, A. Ueber die Verbindungen der Indigogruppe. *Berichte Dtsch. Chem. Ges*. **1882**, *15*, 775–787, https://doi.org/10.1002/cber.188201501167.

30 Friedländer, P. Ueber Schwefelhaltige Analoga Der Indigogruppe. *Berichte Dtsch. Chem. Ges*. **1906**, *39*, 1060–1066, https://doi.org/10.1002/cber.190603901167.

31 Petermayer, C.; Dube, H. Indigoid Photoswitches: Visible Light Responsive Molecular Tools. *Acc. Chem. Res.* **2018**, *51*, 1153–1163, https://doi.org/10.1021/acs.accounts.7b00638.

32 Bakhouch, M.; Es-Sounni, B.; Nakkabi, A.; Yazidi, M. E. Thioaurones: Recent Advances in Synthesis, Reactivity, and Biological Activity. *Mini-Rev. Org. Chem*. **2021**, *18*, 313–327, https://doi.org/10.2174/1570193X17999200719135019.

33 Nguyen, T. B.; Retailleau, P. Cooperative Activating Effect of Tertiary Amine/DMSO on Elemental Sulfur: Direct Access to Thioaurones from 2′-Nitrochalcones under Mild Conditions. *Org. Lett*. **2018**, *20*, 186–189. https://doi.org/10.1021/acs.orglett.7b03547.

34 Nejjari, R.; Bashir, M.; Raji, H.; Es-Sounni, B.; Adardour, M.; Siddique, F.; Bakhouch, M.; Mouzdahir, A.; Benharref, A.; Mazoir, N.; Chtita, S. Semisynthesis and DFT Study of New Michael Adducts Using (E)-A-Atlantone, Isolated from Cedrus Atlantica Essential Oil. *Lett. Org. Chem*. **2024**, *21*, 228-241, https://doi.org/10.2174/0115701786321643240709114001.

35 Nejjari, R.; Raji, H.; Yamari, I.; Laghmari, M.; Touhtouh, J.; Bakhouch, M.; Benharref, A.; Hammani, K.; Benali, T.; Mazoir, N.; Chtita, S. Semisynthesis of New Isoxazolines from (E)-α-Atlantone: Antibacterial, Antifungal Activities, ADME-Tox, Molecular Docking, and Molecular Dynamics Simulations Investigations. *J. Mol. Struct*. **2024**, *1312*, 138579, https://doi.org/10.1016/j.molstruc.2024.138579.

36 Kanzouai, Y.; Laghmari, M.; Yamari, I.; Bouzammit, R.; Bahsis, L.; Benali, T.; Chtita, S.; Bakhouch, M.; Akhazzane, M.; El Kouali, M.; Hammani, K.; Al Houari, G. Chromone-Isoxazole Hybrids Molecules: Synthesis, Spectroscopic, MEDT, ELF, Antibacterial, ADME-Tox, Molecular Docking and MD Simulation Investigations. *J. Biomol. Struct. Dyn*. **2024**, *42*, 6410–6424, https://doi.org/10.1080/07391102.2023.2266022.

37 Chalkha, M.; Nour, H.; Chebbac, K.; Nakkabi, A.; Bahsis, L.; Bakhouch, M.; Akhazzane, M.; Bourass, M.; Chtita, S.; Bin Jardan, Y. A.; Augustyniak, M.; Bourhia, M.; Aboul-Soud, M. A. M.; El Yazidi, M. Synthesis, Characterization, DFT Mechanistic Study, Antimicrobial Activity, Molecular Modeling, and ADMET Properties of Novel Pyrazole-Isoxazoline Hybrids. *ACS Omega* **2022**, *7*, 46731–46744, https://doi.org/10.1021/acsomega.2c05788.

38 Chalkha, M.; Ameziane el Hassani, A.; Nakkabi, A.; Tüzün, B.; Bakhouch, M.; Benjelloun, A. T.; Sfaira, M.; Saadi, M.; Ammari, L. E.; Yazidi, M. E. Crystal Structure, Hirshfeld Surface and DFT Computations, along with Molecular Docking Investigations of a New Pyrazole as a Tyrosine Kinase Inhibitor. *J. Mol. Struct.* **2023**, *1273*, 134255, https://doi.org/10.1016/j.molstruc.2022.134255.

39 Yanai, T.; Tew, D. P.; Handy, N. C. A New Hybrid Exchange–Correlation Functional Using the Coulomb-Attenuating Method (CAM-B3LYP). *Chem. Phys. Lett.* **2004**, *393*, 51–57, https://doi.org/10.1016/j.cplett.2004.06.011.

40 Hehre, W. J. Ab Initio Molecular Orbital Theory. *Acc. Chem. Res.* **1976**, *9*, 399–406, https://doi.org/10.1021/ar50107a003.

41 Schlegel, H. B. Optimization of Equilibrium Geometries and Transition Structures. *J. Comput. Chem*. **1982**, *3*, 214–218, https://doi.org/10.1002/jcc.540030212.

42 Fukui, K. Formulation of the Reaction Coordinate. *J. Phys. Chem*. **1970**, *74*, 4161–4163, https://doi.org/10.1021/j100717a029.

43 Gonzalez, C.; Schlegel, H. B. Improved Algorithms for Reaction Path Following: Higher-order Implicit Algorithms. *J. Chem. Phys*. **1991**, *95*, 5853–5860, https://doi.org/10.1063/1.461606.

44 Frisch, M.J.; Trucks, G.W.; Schlegel, H.B.; Scuseria, G.E.; Robb, M.A.; Cheeseman, J.R.; Scalmani, G.; Barone, V.; Petersson, G.A.; Nakatsuji, H.; Li, X.; Caricato, M.; Marenich, A.; Bloino, J.; Janesko, B.G.; Gomperts, R.; Mennucci, B.; Hratchian, H.P.; Ortiz, J.V.; Izmaylov, A.F.; Sonnenberg, J.L.; Williams-Young, D.; Ding, F.; Lipparini, F.; Egidi, F.; Goings, J.; Peng, B.; Petrone, A.; Henderson, T.; Ranasinghe, D.; Zakrzewski, V.G.; Gao, J.; Rega, N.; Zheng, G.; Liang, W.; Hada, M.; Ehara, M.; Toyota, K.; Fukuda, R.; Hasegawa, J.; Ishida, M.; Nakajima, T.; Honda, Y.; Kitao, O.; Nakai, H.; Vreven, T.; Throssell, K.; Montgomery Jr., J.A.; Peralta, J.E.; Ogliaro, F.; Bearpark, M.; Heyd, J.J.; Brothers, E.; Kudin, K.N.; Staroverov, V.N.; Keith, T.; Kobayashi, R.; Normand, J.; Raghavachari, K.; Rendell, A.; Burant, J.C.; Iyengar, S.S.; Tomasi, J.; Cossi, M.; Millam, J.M.; Klene, M.; Adamo, C.; Cammi, R.; Ochterski, J.W.; Martin, R.L.; Morokuma, K.; Farkas, O.; Foresman, J.B.; Fox, D.J. Gaussian 09. Gaussian, Inc., Wallingford, CT, **2009**.

45 Parr, R. G.; Szentpály, L. v.; Liu, S. Electrophilicity Index. *J. Am. Chem. Soc*. **1999**, *121*, 1922–1924, https://doi.org/10.1021/ja983494x.

46 Ayers, P. W.; Parr, R. G.; Pearson, R. G. Elucidating the Hard/Soft Acid/Base Principle: A Perspective Based on Half-Reactions. *J. Chem. Phys*. **2006**, *124*, 194107, https://doi.org/10.1063/1.2196882.

47 Kresse, G.; Furthmüller, J. Efficiency of Ab-Initio Total Energy Calculations for Metals and Semiconductors Using a Plane-Wave Basis Set. *Comput. Mater. Sci*. **1996**, *6*, 15–50, https://doi.org/10.1016/0927-0256(96)00008-0.

48 Domingo, L.; Pérez, P. The Nucleophilicity N Index in Organic Chemistry. *Org. Biomol. Chem*. **2011**, *9*, 7168–7175, https://doi.org/10.1039/c1ob05856h.

49 Bakhouch, M.; Houari, G. A.; Daoudi, M.; Kerbal, A.; Yazidi, M. E. Michael Addition of Active Methylene Compounds to (Z)-2-Arylidenebenzo[b]Thiophen-3(2H)-Ones. *Mediterr. J. Chem*. **2015**, *4*, 9–17, https://doi.org/10.13171/mjc.4.1.2015.16.02.09.20/elyazidi.

50 Boughaleb, A.; Al Houari, G.; Bennani, B.; Daoudi, M.; Garrigues, B.; Kerbal, A.; El Yazidi, M. Cycloaddition des N-Phényl-C-Arylnitrilimines sur des Dérivés de la 2-Benzylidènebenzo[b]tiophèn-3(2H)-One (Thioaurones). *J. Société Chim. Tunis*. **2010**, *12*, 109–115.

51 Rössing, A. Beobachtungen Über Innere Condensationen Bei Abkömmlingen Des Salicylaldehyds. *Berichte Dtsch. Chem. Ges*. **1884**, *17*, 2988–3010, https://doi.org/10.1002/cber.188401702277.

52 Friedlaender, P. Ueber Thionaphtenderivate und Thioindigo. *Justus Liebigs Ann. Chem*. **1907**, *351*, 390–420, https://doi.org/10.1002/jlac.19073510131.

53 Aggarwal, V. K.; de Vicente, J.; Bonnert, R. V. A Novel One-Pot Method for the Preparation of Pyrazoles by 1,3-Dipolar Cycloadditions of Diazo Compounds Generated in Situ. *J. Org. Chem*. **2003**, *68*, 5381–5383, https://doi.org/10.1021/jo0268409.